HHS Public Access

Author manuscript

Soft Matter. Author manuscript; available in PMC 2015 November 28.

Published in final edited form as:

Soft Matter. 2014 November 28; 10(44): 8821–8828. doi:10.1039/c4sm01784f.

Organized Assemblies of Colloids Formed at the Poles of Micrometer-Sized Droplets of Liquid Crystal

Xiaoguang Wang[a], **Daniel S. Miller**[a], **Juan J. de Pablo**[b], and **Nicholas L. Abbott**[a]

Nicholas L. Abbott: abbott@engr.wisc.edu

[a]Department of Chemical and Biological Engineering, University of Wisconsin-Madison, 1415 Engineering Drive, Madison, Wisconsin 53706-1607, USA

[b]Institute for Molecular Engineering, University of Chicago, 5801 South Ellis Avenue Chicago, Illinois 60637, USA

Abstract

We report on the formation of organized assemblies of 1 μm-in-diameter colloids (polystyrene (PS)) at the poles of water-dispersed droplets (diameters 7 - 20 μm) of nematic liquid crystal (LC). For 4-cyano-4′-pentylbiphenyl droplets decorated with two to five PS colloids, we found 32 distinct arrangements of the colloids to form at the boojums of bipolar droplet configurations. Significantly, all but one of these configurations (a ring comprised of five PS colloids) could be mapped onto a local (non-close packed) hexagonal lattice. To provide insight into the origin of the hexagonal lattice, we investigated planar aqueous—LC interfaces, and found that organized assemblies of PS colloids did not form at these interfaces. Experiments involving the addition of salts revealed that a repulsive interaction of electrostatic origin prevented formation of assemblies at planar interfaces, and that regions of high splay near the poles of the LC droplets generated cohesive interactions between colloids that could overcome the repulsion. Support for this interpretation was obtained from a model that included (i) a long-range attraction between adsorbed colloids and the boojum due to the increasing rate of strain (splay) of LC near the boojum (splay attraction), (ii) an attractive inter-colloid interaction that reflects the quadrupolar symmetry of the strain in the LC around the colloids, and (iii) electrostatic repulsion between colloids. The model predicts that electrostatic repulsion between colloids can lead to a ∼1,000 k_BT energy barrier at planar interfaces of LC films, and that the repulsive interaction can be overcome by splay attraction of the colloids to the boojums of the LC droplets. Overall, the results reported in this paper advance our understanding of the directed assembly of colloids at interfaces of LC droplets.

Introduction

Assemblies formed by colloids at liquid—liquid[1-3] and liquid—gas[4-8] interfaces can serve as models for a range of molecular phenomena,[1, 2] including molecular self-assembly. They can also provide a means of stabilizing liquid—liquid emulsions[9-11] and synthesizing materials with tunable mechanical, [12, 13] optical, [14, 15] or electronic properties.[16, 17] When

Correspondence to: Nicholas L. Abbott, abbott@engr.wisc.edu.

dealing with isotropic liquids, inter-colloid forces that act parallel to the interface include capillary,[18, 19] dipolar electrostatic,[20-23] and van der Waals forces.[7] If one of the liquids is a liquid crystal (LC), however, the elasticity of the LC phase as well as topological defects formed within the LC can generate additional types of inter-colloid interactions.[24-36] Significantly, LC-mediated interactions have unusual symmetries, including dipolar or quadrupolar symmetries, [24-29] which leads to the formation of chains or hexagonal arrays of colloids.[33, 34] In addition, inter-colloid interactions have been proposed to arise from a coupling between the elasticity of LCs and capillary interactions (so-called elastocapillary interactions).[30-32]

While ordered assemblies of colloids have been widely investigated at planar interfaces of LCs, only recently have assemblies of colloids on the curved interfaces of LC droplets been reported.[34-36] Specifically, we reported on the adsorption of pairs of colloids onto LC microdroplets (diameters ranging from 7 to 20 μm) in a bipolar configuration (see Fig. 1 below) and found the colloids to adopt one of two arrangements – in one arrangement, a single colloid was positioned at each of the two diametrically opposed surface defects (*i.e.*, "boojums");in the second arrangement both colloids were localized at a single boojum.[35] We showed that it was also possible to polymerize the LC droplets with colloids positioned at their poles, thus leading to formation of "patchy" LC particles (spherical and non-spherical).[35] Through a combination of experiment and simulation, we confirmed that the colloids localized at the boojums to eliminate the energetic cost of the defect core (estimated to have a size of ~10 nm[37]) as well as regions of high strain in the LC in the vicinity of the defect core.[36] In this paper, we move beyond our past studies to investigate formation of assemblies of larger numbers of colloids near the poles of LC droplets. In this context, we note that Gharbi and coworkers recently reported on assemblies formed by 4 μm-in-diameter silica colloids, treated to induce homeotropic anchoring of LC, on the surfaces of large (150 to 250 μm-in-diameter) bipolar LC droplets dispersed in an aqueous solution of polyvinyl alcohol.[34] Because the LC droplets used in their study were large compared to the colloid size, they observed organizations of the colloids that were closely related to those observed at planar LC interfaces (linear chains arising from dipolar interactions were reported).[33] In contrast, in the study reported in this paper, we use 1 μm-in-diameter colloids and LC droplets that are less than 20 μm-in-diameter, and demonstrate that in this size range, the inter-colloid forces on the droplet interface lead to assemblies that are not observed to form on planar LC interfaces.

Experimental

Materials

1 μm-in-diameter fluorescently labelled polystyrene particles (PS colloids; λ_{exc}= 480 nm/λ_{em}= 520 nm) were purchased from Bangs Laboratories (Fishers, IN). Sodium chloride (NaCl) was purchased from Sigma Aldrich (St. Louis, MO). Polyimide (PI 2556) was purchased from HD Microsystems (Parlin, NJ). 4-cyano-4′-pentylbiphenyl (5CB) was obtained from EM Sciences (New York, NY). Deionization of a distilled water source was performed with a Milli-Q system (Millipore, Bedford, MA).

Preparation of liquid crystal (LC)-in-water emulsions

Emulsions formed from LC droplets dispersed in water (so-called LC-in-water emulsions) were prepared according to previously published methods.[35, 36] Briefly, the emulsions were prepared by emulsifying 4 μL 5CB in 1.98 mL of an aqueous phase using a homogenizer (T25 digital ULTRA-TURRAX) equipped with a S25 N-10G dispersing element (IKA) for 30 s at 6,500 rpm. This procedure resulted in a population of droplets in the bipolar configuration. The emulsions were prepared in glass vials (diameter of 19 mm, height of 51 mm).

Adsorption of PS colloids onto the surfaces of LC droplets

PS colloids were adsorbed onto the surfaces of the LC droplets through addition of 20 μL of a 1% wt/v PS colloids dispersion to 1.98 mL of a LC-in-water emulsion, followed by homogenization at 6,500 rpm. The duration of homogenization was 30 s, 45 s, 60 s, 90 s, or 300 s for experiments with two, three and four, five, six and seven, or many (more than seven) adsorbed colloids, respectively.

Preparation of PS colloid-decorated planar aqueous—5CB interfaces

Glass slides coated with a PI film (rubbed) were prepared according to previous published methods.[33, 35] A film of 5CB with an approximately flat interface was prepared by filling the pores of a 20 μm-thick gold-coated specimen grid supported on a PI-treated glass slide. The system was then submerged in water. Finally, we added 2 mL of a 0.005% wt/v PS colloid dispersion to the aqueous phase above the LC films and allowed the colloids to sediment onto the aqueous—LC interface.

Bright field (BF), polarized light (PL), and fluorescence (Fluo) microscopy

To characterize assemblies of PS colloids that formed at the surfaces LC droplets, a 50 μL volume of the LC emulsion was dispensed onto a glass coverslip. Next, the LC droplets were imaged using an Olympus IX71 inverted epifluorescence microscope (Center Valley, PA) equipped with a 100× oil-immersion objective, crossed polarizers, mercury lamp, and Chroma filter (457 nm ≤ λ_{exc} ≤ 502 nm, and 510 nm ≤ λ_{em} ≤ 562 nm). BF, PL, and Fluo micrographs of LC-in-water emulsions were collected with a Hamamatsu 1394 ORCAER CCD camera (Bridgewater, NJ) connected to a computer and controlled through SimplePCI imaging software (Compix, Inc., Cranberry Twp., NJ). BF micrographs were collected by removing the polarizer from the optical path of the microscope. BF, PL, and Fluo micrographs of assemblies of PS colloids that formed at planar aqueous—5CB interfaces were captured using the same microscope.

Results

The goal of our first set of experiments was to characterize the packing arrangements exhibited by 1 μm-in-diameter fluorescent PS colloids adsorbed to the surfaces of droplets of nematic 5CB in the bipolar configuration. The 5CB-in-water emulsions with droplets in the bipolar configuration were prepared by dispersing 5CB in pure water, and homogenizing the mixture for 30 s. This procedure resulted in a polydisperse emulsion with LC droplets with diameters ranging from 1 - 40 μm. In our experiments, we focused our observations on LC

droplets with diameters between 7 - 20 μm. After formation of the LC emulsions, the PS colloids, which induce a planar anchoring of nematic 5CB, were adsorbed to the surfaces of the LC droplets through addition of a 1 % wt/v dispersion of the colloids, followed by homogenization. We found that homogenization for 30 s led to a population of LC droplets within which a significant number of droplets had two colloids adsorbed to their surfaces. Here we briefly summarize results obtained with two adsorbed colloids as context to our observations involving larger numbers of colloids.

Fig. 1B shows Fluo, BF and PL micrographs of a bipolar 5CB droplet with two PS colloids adsorbed to the droplet surface. A schematic illustration of the configuration of the LC within the droplet is also shown to the right of the micrographs. In the bipolar configuration, LC is aligned tangential to the droplet surface, and two boojum defects are present at diametrically opposite ends of the droplet.[38-45] By comparing the Fluo micrograph to the BF and PL micrographs in Fig. 1B, it is evident that the Fluo signal from the two adsorbed PS colloids coincides with the location of one of the two boojums (as we have previously reported[35, 36]).

Before describing results involving three or more colloids adsorbed to the surfaces of the LC droplets, we make four guiding statements. First, below we present only the Fluo micrographs of the colloid-decorated LC droplets because the Fluo micrographs clearly reveal the packing arrangements of the colloids. However, we emphasized that we captured BF and PL micrographs for all droplets to confirm that the colloids were localized in the vicinity of boojum defects of a bipolar configuration (*i.e.*, in the vicinity of a pole of the droplets). Second, although the colloids were observed to accumulate in the vicinity of the poles of the droplets, the scattering of light from the interfaces of the colloids and the optical resolution of our microscope (∼500 nm) did not allow us to determine the exact positions of the colloids relative to the boojums. In the description of our experimental results below, for brevity, we state that the colloids accumulate at a pole of the droplets. Third, we observed assemblies of colloids to form at diametrically opposite poles of bipolar LC droplets with equal probability (see Fig. S1 of ESI[†]). Finally, all packing arrangements of adsorbed colloids were observed to form within 1 min and to persist for at least six hours (much longer than the typical time for reorganization of the colloids on the surface of LC droplet (∼ 1 min for 10 μm-in-radius LC droplet)[46]). The colloids did not rearrange into different packing arrangements over six hours of equilibration.

By increasing the duration of homogenization of the colloids and LC droplets to 45 s, we obtained an increasing population of droplets within each emulsion that had three or four colloids adsorbed to their surfaces. For droplets with three colloids adsorbed at a pole, we observed three packing arrangements, each occurring with a different frequency, as shown in Fig. 1C. When droplets with four colloids at their poles were observed, seven different

[†]Electronic Supplementary Information (ESI) available: Distribution of the positions of adsorbed polystyrene colloids between the two boojums of the bipolar configuration of LC droplets; Optical characterization of the anchoring of LC on PS colloids adsorbed at planar aqueous—LC interface; Effect of contrast enhancement on fluorescence images; Spacing between PS colloids adsorbed at the surface of LC droplets in the presence of salt; Role of nematic order in the formation of arrays of colloids adsorbed at the surface of LC droplets; Derivation of the expression for splay attraction; Contact angle for PS colloids adsorbed at the surfaces of LC droplets; Measurement of surface charge density of PS colloids; Analysis of the relative stabilities of packing arrangements of five PS colloids on the surfaces of bipolar LC droplets. See DOI: 10.1039/b000000x/

arrangements were seen, again with different frequencies, as shown in Fig. 1D. Inspection of Fig. 1 reveals that, while extended assemblies were observed (*e.g.*, chain-like assemblies), the packing arrangement that maximized colloid— colloid contacts tended to be observed with the highest frequency. We return to this observation below.

Following characterization of droplets decorated with three and four adsorbed PS colloids, we increased further the homogenization period to 60 s, to increase the likelihood of obtaining 5CB droplets with five PS colloids adsorbed at a pole. For such droplets, twenty-one unique configurations were observed, as shown in Fig. 2. Similar to the case of three or four adsorbed colloids, we observed compact assemblies with the highest frequency. Interestingly, the second most frequently observed arrangement was an arrangement that comprised a ring of colloids (top of the second column in Fig. 2).

To characterize the symmetry of the packing arrangements of PS colloids on the surfaces of 5CB droplets, we next quantified the angles and spacings between adjacent PS colloids. The angles defined by adjacent colloids within the observed arrangements are shown in Fig. 3A and 3B, respectively. Inspection of Fig. 3 reveals that the angles are consistent with the geometry of a right hexagon and right pentagon, respectively. In addition, the center-to-center distance between adjacent colloids was measured to be 1.17 ± 0.06 μm, which indicates that the PS colloids with diameters of 1.01 ± 0.01 μm are not close packed (we note that we measured the diameters of 30 PS colloids in Fluo micrographs to obtain the average diameter and the error represents the standard deviation). From this analysis, we conclude that the packing arrangements of PS colloids shown in Figs. 1 and 2 followed a hexagonal lattice, with the exception of the pentamer ring pattern observed for five colloids. We note here that the pentamer ring pattern has not been previously reported for assemblies of colloids at aqueous—LC interfaces.

We sought to provide insight into the relative stabilities of the various hexagonal and pentagonal packing arrangements by characterizing the frequency (F) with which we observed the various packing arrangements as a function of the total number of nearest neighbor colloid—colloid contacts (N) within each arrangement. To illustrate our analysis, we use LC droplets with five PS colloids (Fig. 2) as a representative example. Four values of N (4, 5, 6 and 7) describe the arrangements shown in Fig. 2. The frequency histogram for these N values, shown in Fig. 4A, reveals that the arrangements corresponding to $N = 5$ are observed with the highest frequency. However, the results in Fig. 4A do not directly reflect the relative energies of the packing arrangements because a smaller number of arrangements is possible for assemblies of colloids with higher N (note that only one arrangement, a hexagonal array that maximizes N, is observed for $N = 7$). To account for the multiplicity (M) of ways to arrange five colloids into an assembly with $N = 4$, 5, or 6, we normalized F by M. Fig. 4B shows that F/M for $N = 7$ is at least three times larger than F/M for all other N values, which suggests that the assembly with $N = 7$ is the energetically most stable arrangement. We end this discussion by noting that we also attempted to quantify the relative energies of arrangements of five colloids with different N by assuming that the frequency distribution was described by a Boltzmann distribution (see Fig. S8 and the accompanying text of ESI[†]). Although the analysis supported our proposal that the assembly with $N = 7$ is the energetically most stable arrangement, it also predicted the different

arrangements to be separated by very small energy differences (of order k_BT). The small energy difference is not consistent with our observation of long-lived (see above) arrangements of the colloids. We therefore conclude that the distribution of packing arrangements ($F(N)$) observed in our experiments are likely influenced by kinetic barriers (additional discussion below).

Next, we investigated assemblies formed by larger numbers of PS colloids adsorbed at the surfaces of bipolar LC droplets. Here we comment that LC droplets decorated with many colloids are of potential technological interest because, for example, as noted in the Introduction, colloids can stabilize LC-in-water emulsions (*i.e.*, to enable design of stimuli-responsive LC emulsions)[42, 47] and they can lead to Janus-like polymer microparticles.[35]Fig. 5 shows some of the packing arrangements most frequently observed for droplets with six or seven adsorbed colloids. As was the case for fewer than six colloids, the most frequently observed packing arrangements possess a hexagonal symmetry. Assemblies with more than seven adsorbed colloids are shown in Fig. 5C. When many colloids were adsorbed to the LC droplets, we observed both the hexagonal array and pentamer ring pattern described above (both patterns are marked in Fig. 5C). We note here that a uniform hexagonal array of PS colloids cannot form on the surface of a LC droplet at complete coverage due to the curvature of the surface of the LC droplet. In contrast, the Caspar and Klug “quasi-equivalence” principle often used to describe the packing of protein subunits on the spherical shells of viruses states that an icosahedral pattern constructed from pentamers and hexamers generates the maximum enclosed volume for a shell.[48-51] We speculate that complete coverage of the LC droplets by PS colloids may lead to an icosahedral packing arrangement analogous to that of viruses.

We performed three additional experiments to provide insight into the origin of the hexagonal arrays of colloids formed at the poles of bipolar LC droplets. First, we investigated the role of nematic order by heating the LC droplets into the isotropic phase. The PS colloids were observed to dissociate from the initial hexagonal array upon heating into the isotropic phase (see Fig. S5). We attribute the observed tendency of the colloids to move apart to electrostatic repulsion (see below). From this result, we conclude that the strained nematic phase of the LC plays a key role in driving the formation of hexagonal arrays of PS colloids at the poles of bipolar LC droplets.

Second, we investigated the role of interface curvature on array formation. Specifically, the PS colloids used in the droplet experiments described above were sedimented onto planar aqueous—LC interfaces of 20 μm-thick films of 5CB (see Fig. S2 of ESI† for a schematic illustration of the film which was supported on rubbed PI to promote a uniform planar alignment of 5CB; the concentration of colloids added to the aqueous phase was 0.005 % wt/v). Surprisingly, and in contrast to LC droplets, the PS colloids did not spontaneously assemble into organized arrays at the planar aqueous—LC interface (even after several days; Fig. 6A). At first we interpreted the lack of organization exhibited by the colloids as a consequence of weak anchoring of the LC on the surfaces of the colloids, thus preventing topological dipole—dipole or quadrupole—quadrupole interactions between colloids (see Introduction and below).[24-29] However, PL micrographs of isolated colloids revealed an optical signature consistent with quadrupolar symmetry and strain-induced formation of two

diametrically opposite boojum defects at the surface of a colloid (see Fig. S2 of ESI†).[28, 35, 52] When combined, these various observations led us to conclude that the droplet geometry was necessary to obtain the hexagonal array of colloids (at the conditions reported above), and that a repulsive interaction kept the colloids separated at planar interfaces (preventing quadrupole—quadrupole elastic interactions from generating ordered assemblies of colloids). We emphasize here that the regions of the aqueous—LC interface used in our study possessed a uniform azimuthal alignment (and thus were free of defects) because the LC film was supported on the rubbed polyimide surface.

The absence of ordering exhibited by PS colloids adsorbed to the aqueous interfaces of isotropic 5CB droplets (Fig. S5B) and planar films of nematic 5CB (Fig. 6A), when combined with the observed non-close packed arrangement of colloids on the surfaces of bipolar 5CB droplets, points to the existence of a repulsive interaction between PS colloids. We hypothesized that the origin of the repulsive interaction was electrostatic. To test this hypothesis, 5CB droplets with PS colloids adsorbed at their surfaces were prepared in the presence of 1 mM NaCl. Consistent with screening of electrostatic repulsion between PS colloids at the droplet interface, the center-to-center distance between adjacent colloids on the LC droplets was measured to decrease from 1.17 ± 0.06 μm in the absence of salt to 1.07 ± 0.04μm in the presence of NaCl (see Fig. S4 of ESI†). To summarize, the results of these three experiments led us to conclude that two conditions necessary for formation of hexagonal arrays of colloids were: (i) nematic order of 5CB; and (ii) interfacial curvature (droplets).

Discussion

The experimental results reported above provide qualitative insight into the origin of the hexagonal arrays of PS colloids formed in the vicinity of boojum defects of water-dispersed bipolar 5CB microdroplets. Specifically, they led us to hypothesize that three interactions underlie formation of the hexagonal arrays: (i) a long-range attraction of the PS colloids towards the boojum defects, at which splay distortions of the LCs are at a maximum (splay attraction); (ii) inter-colloid quadrupole—quadrupole elastic interactions (the result of a quadrupolar topological defect structure), and (iii) electrostatic repulsion between colloids. Here we present a simple model that accounts for each interaction, and we test predictions that emerge from the model against our experimental observations. We comment here that our simple model focuses on pairwise interactions between colloids at these interfaces, although some studies suggest multibody effects may be important.[5, 31, 33]

The first term of our model captures splay attraction and is expressed as:

$$U_{splay} = -\frac{8}{3}\pi K\frac{a^3}{d^2} \quad (1)$$

in which K is the elastic constant of the LC (10^{-11} N)[53] and a is the radius of the PS colloid (0.5 μm). Because we consider pairwise interactions between colloids, we take d to be the center-to-center distance between two PS colloids, one of which is fixed at the location of a boojum defect (*i.e.*, the location of maximum splay; see Fig. S6 of ESI†). Thus, eqn (1)

estimates the energy gain from replacement of strained LC as the second colloid moves towards a first colloid positioned at the boojum (see ESI† for the derivation). As described in the ESI, eqn (1) is an approximation to U_{splay} as, for example, it does not include curvature strain (bending) due to the constraints imposed by the curved interface of the LC.

The second term in our model is a quadrupole—quadrupole elastic interaction between adsorbed PS colloids and is evaluated as:

$$U_{quad}=\frac{\pi W^2 a^8}{30Kd^5}\left(1-\frac{Wa}{56K}\right)(9+20\cos(2\theta)+35\cos(4\theta)) \quad (2)$$

in which W is the surface anchoring coefficient (10^{-4} J/m^2),[54, 55] and θ is the angle formed between the LC director and a line connecting the center of mass of each colloid.[29] We note here that the magnitude and sign of the quadrupole—quadrupole interaction depends on θ and that for the purposes of this paper θ was fixed at 49.1°to obtain the maximum attractive interaction.

The third and final term in our model is an electrostatic repulsion between colloids, which is evaluated as:

$$U_{elec}=\frac{2\varepsilon_{5CB}\pi\alpha_W^2\sigma^2a^2\sin2\gamma}{\varepsilon_0\varepsilon_W^2\kappa^4d^3} \quad (3)$$

in which ε_0 is the permittivity of vacuum (8.85×10^{-12} C^2/J·m),[56] ε_w is the dielectric constant of water (78),[56] ε_{5CB} is the average dielectric constant of 5CB (11),[57, 58] α_W is the extent of dissociation of surface charge groups (0.25), σ is the surface charge density (0.06 e$^-$/nm^2, see ESI† for details), γ is the contact angle at the aqueous—5CB interface (95°, see ESI† for details), and κ is the Debye-Huckel parameter ($1/\kappa$ is the Debye screening length).[59] Eqn (3) describes the effective dipole—dipole interaction between PS colloids at the aqueous—LC interface that results from the asymmetry of the ionic atmosphere surrounding the colloids in water.[58] For simplicity, in the above model, the anisotropy of the dielectric properties of 5CB is neglected.

Using the above-described model, we calculated the free energy as a function of the center-to-center distance between PS colloids adsorbed to either the aqueous—LC interface of a bipolar LC droplet (all three terms in the model) or a planar LC film (U_{quad} and U_{elec} only). Fig. 7 shows predictions of the model. Interestingly, for the case of colloids adsorbed at the planar aqueous—LC interface (solid line), our model predicts a ~1,000 k_BT energy barrier due to electrostatic repulsion. However, no such barrier was observed for colloids adsorbed at the surface of the bipolar LC droplet (dashed line), indicating that the electrostatic energy barrier preventing colloidal assembly on the planar interface was overcome by splay attraction on the LC droplet surface. Overall, this simple simulation captures a key difference in the behavior of PS colloids at the interfaces of LC droplets or films.

Next, we determined if the electrostatic energy barrier for colloidal assembly on a planar LC film, as shown in Fig. 7, would vanish upon addition of salt to the aqueous phase; Fig. S4 of ESI[†]). Fig. 7 reveals that the energy barrier predicted by the model indeed disappears in the presence of 1 mM NaCl (dotted line). To test this prediction in an experiment, we sedimented PS colloids onto the aqueous—LC interface of a 20 μm-thick film of 5CB with a uniform planar alignment in the presence of 1 mM NaCl. In agreement with our prediction, Fig. 6B reveals that chain-like assemblies of PS colloids formed at the interface (see below). The result of this simple experiment further validates the ability of our simple model to capture key behaviors of colloids at aqueous—LC interfaces.

We end this discussion by commenting on an additional difference that we observe between the ordered assemblies of colloids formed on the surfaces of bipolar LC droplets and planar LC films. On planar LC interfaces, we observed chains of PS colloids (Fig. 6B). The chaining is a consequence of the quadrupole—quadrupole elastic interactions between the colloids.[29] In contrast, on droplets we did not observe chains, but rather hexagonal assemblies of colloids that maximized colloid—colloid contacts. The compact nature of the hexagonal assemblies (as opposed to chains) on the LC droplets is caused by the splay deformation in the LC droplets, which tends to concentrate the colloids near the poles of the droplets. In summary, the difference between the assemblies observed on the aqueous—LC interfaces of planar films and bipolar LC droplets further highlights the importance of splay attraction in directing formation of colloidal assemblies on the surfaces of LC microdroplets. We speculate that the controlled introduction of defects into the interfaces of planar LC films (such as by using flow fields) can also be used to direct the formation of assemblies of colloids in a manner analogous to that reported in this paper.

Conclusions

Overall, the results reported in this paper advance our understanding of colloidal assemblies formed on curved LC interfaces. We reveal that three key interactions underlie the organized assemblies formed by 1 μm-in-diameter PS colloids at the curved surfaces of water-dispersed nematic LC microdroplets in the bipolar configuration: (i) a long-range attraction of the adsorbed colloids to boojums at which splay distortion of the LC is at a maximum (splay attraction), (ii) inter-colloid quadrupole— quadrupole elastic interactions (the result of a quadrupolar topological defect structure), and (iii) electrostatic repulsion between colloids. These three interactions promote formation of hexagonal arrays of colloids in the vicinity of boojum defects. In contrast, for the case of colloids at the aqueous—LC interface of a LC film with a uniform planar alignment, the splay attraction is absent and the electrostatic repulsion keeps colloids separated under conditions of low ionic strength of the aqueous phase. However, addition of simple salt to the aqueous phase can screen the repulsion and leads to chaining of colloids at the interface. Thus, the influence of splay attraction on the curved LC droplet interface is two-fold. It both overcomes repulsive interactions to promote the ordering of colloids on the surfaces of LC droplets, and plays a key role in determining the morphology of the assembly formed.

The results reported in this paper also provide guidance for the design of functional soft materials based on LC droplet-templated colloidal assemblies. In particular, our study

reveals that unusual arrangements of colloids (not observed on droplets of isotropic liquids) can be accessed by assembling colloids on the surfaces of bipolar LC droplets (*e.g.*, open hexagonal or pentamer ring structures). These arrangements and the properties associated with them will be investigated further in a future study, but we point out here that the observation of a pentamer ring pattern suggests that synthetic versions of the shells of sphere-like viruses might be realized through the use of LC droplets as templates.

Supplementary Material

Refer to Web version on PubMed Central for supplementary material.

Acknowledgments

This work was primarily supported by NSF through DMR-1121288 (Materials Research Science and Engineering Center), the Army Research Office (W911NF-11-1-0251 and W911NF-10-1-0181), and the National Institutes of Health (CA108467, CA105730, AI092004.). Acknowledgment of support related to simulations is made to the Department of Energy, Basic Energy Sciences, Biomaterials Program (DESC0004025). The authors thank Dr. Jonathan K. Whitmer, Tyler F. Roberts, Reza Abbasi, and Emre Bukusoglu for helpful discussions.

References

1. Park BJ, Pantina JP, Furst EM, Oettel M, Reynaert S, Vermant J. Langmuir. 2008; 24:1686–1694. [PubMed: 18201109]
2. Bowden NB, Weck M, Choi IS, Whitesides GM. Accounts of Chemical Research. 2001; 34:231–238. [PubMed: 11263881]
3. Hunter TN, Pugh RJ, Franks GV, Jameson GJ. Advanced in Colloid and Interface Science. 2008; 137:57–81.
4. Nazarenko VG, Nych AB, Lev BI. Physical Review Letters. 2001; 87:075504. [PubMed: 11497900]
5. Nych AB, Ognysta UM, Pergamenshchik VM, Lev BI, Nazarenko VG, Musevic I, Skarabot M, Lavrentovich OD. Physical Review Letters. 2007; 98:057801. [PubMed: 17358900]
6. Oettel M, Dietrich S. Langmuir. 2008; 24:1425–1441. [PubMed: 18179271]
7. Onoda GY. Physical Review Letters. 1985; 55:226. [PubMed: 10032034]
8. Assoud L, Ebert F, Keim P, Messina R, Maret G, Löwen H. Physical Review Letters. 2009; 102:238301. [PubMed: 19658976]
9. Binks BP, Murakami R. Nature Materials. 2006; 5:865–869. [PubMed: 17041582]
10. Giermanska-Kahn J, Schmitt V, Binks B, Leal-Calderon F. Langmuir. 2002; 18:2515–2518.
11. Vignati E, Piazza R, Lockhart TP. Langmuir. 2003; 19:6650–6656.
12. Aussillous P, Quéré D. Nature. 2001; 411:924–927. [PubMed: 11418851]
13. Meeker S, Poon W, Crain J, Terentjev E. Physical Review E. 2000; 61:R6083.
14. Hosoki K, Tayagaki T, Yamamoto S, Matsuda K, Kanemitsu Y. Physical Review Letters. 2008; 100:207404. [PubMed: 18518579]
15. Kim B, Tripp SL, Wei A. Materials Research Society Symposium Proceedings. 2002; 676:Y6. 1–Y6. 4.
16. Kim J, Lee D. Journal of the American Chemical Society. 2006; 128:4518–4519. [PubMed: 16594657]
17. Velev OD, Kaler EW. Advanced Materials. 2000; 12:531–534.
18. Kralchevsky PA, Nagayama K. Advances in Colloid and Interface Science. 2000; 85:145–192. [PubMed: 10768480]
19. Botto L, Lewandowski EP, Cavallaro M, Stebe KJ. Soft Matter. 2012; 8:9957–9971.
20. Pieranski P. Physical Review Letters. 1980; 45:569–572.

21. Frydela D, Oettel M. Physical Chemistry Chemical Physics. 2011; 13:4109–4118. [PubMed: 21229151]
22. Wirth CL, Furst EM, Vermant J. Langmuir. 2014; 30:2670–2675. [PubMed: 24598009]
23. Uppapalli S, Zhao H. Soft Matter. 2014; 10:4555–4560. [PubMed: 24817608]
24. Poulin P, Stark H, Lubensky T, Weitz D. Science. 1997; 275:1770–1773. [PubMed: 9065396]
25. Lubensky T, Pettey D, Currier N, Stark H. Physical Review E. 1998; 57:610.
26. Ruhwandl R, Terentjev E. Physical Review E. 1997; 55:2958.
27. Musevic I, Skarabot M, Tkalec U, Ravnik M, Zumer S. Science. 2006; 313:954–958. [PubMed: 16917058]
28. Stark H. Physics Reports. 2001; 351:387–474.
29. Smalyukh II, Lavrentovich OD, Kuzmin AN, Kachynski AV, Prasad PN. Physical Review Letters. 2005; 95:157801. [PubMed: 16241762]
30. Smalyukh II, Chernyshuk S, Lev BI, Nych AB, Ognysta U, Nazarenko VG, Lavrentovich OD. Physical Review Letters. 2004; 93:117801. [PubMed: 15447380]
31. Oettel M, Domngez A, Tasinkevych M, Dietrich S. The European Physical Journal E. 2009; 28:99–111.
32. Gharbi MA, Nobili M, In M, Prévot G, Galatola P, Fournier JB, Blanc C. Soft Matter. 2011; 7:1467–1471.
33. Koenig GM, Lin IH, Abbott NL. Proceedings of the National Academy of Sciences of the United States of America. 2010; 107:3998–4003. [PubMed: 20133750]
34. Gharbi MA, Nobili M, Blanc C. Journal of Colloid and Interface Science. 2014; 417:250–255. [PubMed: 24407684]
35. Mondiot F, Wang X, de Pablo JJ, Abbott NL. Journal of the American Chemical Society. 2013; 135:9972–9975. [PubMed: 23600692]
36. Whitmer JK, Wang X, Mondiot F, Miller DS, Abbott NL, Pablo Jd. Physical Review Letters. 2013; 111:227801. [PubMed: 24329470]
37. Stark H. Physics Reports. 2001; 351:387–474.
38. Berggren E, Zannoni C, Chiccoli C, Pasini P, Semeria F. Physical Review E. 1994; 50:2929–2939.
39. Drzaic, PS. Liquid Crystal Dispersions. World Scientific; River Edge, NJ, USA: 1995.
40. Gupta JK, Zimmerman JS, de Pablo JJ, Caruso F, Abbott NL. Langmuir. 2009; 25:9016–9024. [PubMed: 19719217]
41. Meyer RB. Physical Review Letters. 1969; 22:918.
42. Miller DS, Wang X, Abbott NL. Chemistry of Materials. 2013; 26:496–506. [PubMed: 24882944]
43. Ondris-Crawford R, Boyko EP, Wagner BG, Erdmann JH, Zumer S, Doane JW. Journal of Applied Physics. 1991; 69:6380–6386.
44. Prischepa OO, Shabanov AV, Zyryanov VY. JETP Letters. 2004; 79:257–261.
45. Volovik GE, Lavrentovich OD. Zhurnal Eksperimentalnoi I Teoreticheskoi Fiziki. 1983; 85:1997–2010.
46. Wang X, Miller DS, de Pablo JJ, Abbott NL. Advanced Functional Materials. 201410.1002/adfm.201400911
47. Carlton RJ, Hunter JT, Miller DS, Abbasi R, Mushenheim PC, Tan L, Abbott NL. Liquid Crystal Reviews. 2013; 1:1–23.
48. Berger B, Shor PW, Tucker-Kellogg L, King J. Proceedings of the National Academy of Sciences. 1994; 91:7732–7736.
49. Marzec CJ, Day LA. Biophysical Journal. 1993; 65:2559–2577. [PubMed: 8312492]
50. Zandi R, Reguera D, Bruinsma RF, Gelbart WM, Rudnick J. Proceedings of the National Academy of Sciences of the United States of America. 2004; 101:15556–15560. [PubMed: 15486087]
51. Caspar DLD, Klug A. Quantitative Biology. 1962; 27:1–24. [PubMed: 14019094]
52. Poulin P, Weitz D. Physical Review E. 1998; 57:626.
53. Kléman, M.; Lavrentovich, OD. Soft Matter Physics: An Introduction. Springer; New York, NY, USA: 2003.

54. Rapini A, Papoular M. Journal de Physique Colloques. 1969; 30:C4–54. C54–56.
55. Seo DS, Muroi K, Isogami T, Matsuda H, Kobayashi S. Japanese Journal of Applied Physics. 1992; 31:2165–2169.
56. Israelachvili, JN. Intermolecular and Surface Forces. Academic Press London; San Diego, CA, USA: 1991.
57. Carlton RJ, Gupta JK, Swift CL, Abbott NL. Langmuir. 2012; 28:31–36. [PubMed: 22106820]
58. Miller DS, Carlton RJ, Mushenheim PC, Abbott NL. Langmuir. 2013; 29:3154–3169. [PubMed: 23347378]
59. Aveyard R, Binks B, Clint J, Fletcher P, Horozov T, Neumann B, Paunov V, Annesley J, Botchway S, Nees D. Physical Review Letters. 2002; 88:246102. [PubMed: 12059318]

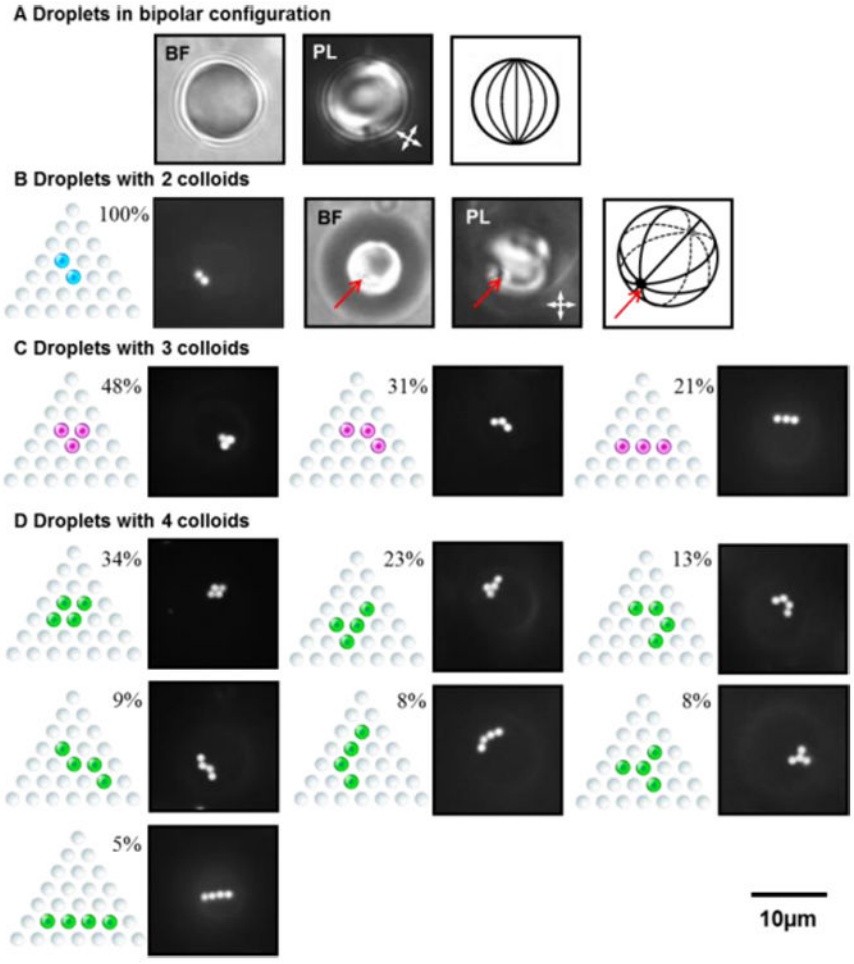

Fig. 1.

Packing arrangements observed for 1 μm-in-diameter, fluorescent PS colloids adsorbed to the poles of nematic 5CB droplets in bipolar configurations. (A) Bright field (BF) and polarized light (PL) micrographs of a droplet of 5CB in a bipolar configuration, as well as a schematic illustration of the bipolar configuration. Note that in the bipolar configuration, the LC is aligned tangentially to the droplet surface and two diametrically opposite point defects (boojums) are present at the poles of the droplets. (B) (left to right), for two PS colloids, schematic illustration, fluorescence micrograph of two colloids, and BF and PL micrographs and a schematic illustration of a 5CB droplet. (C and D) Arrangements are shown for (C) three and (D) four colloids. For each arrangement, we show a schematic illustration of the arrangement (left) and a fluorescence micrograph (right). The orientation of the crossed polarizers in PL micrographs is indicated by the white double-headed arrows. The red arrows indicate the location of the boojum defect at which the colloids are adsorbed. The percentages of droplets in each arrangement is expressed to the right of each schematic illustration, and was calculated from analysis of (B) 121, (C) 175 or (D) 180 droplets in 5 independent experiments. In Fluo micrographs, the contrast is enhanced to highlight the arrangements of colloids.

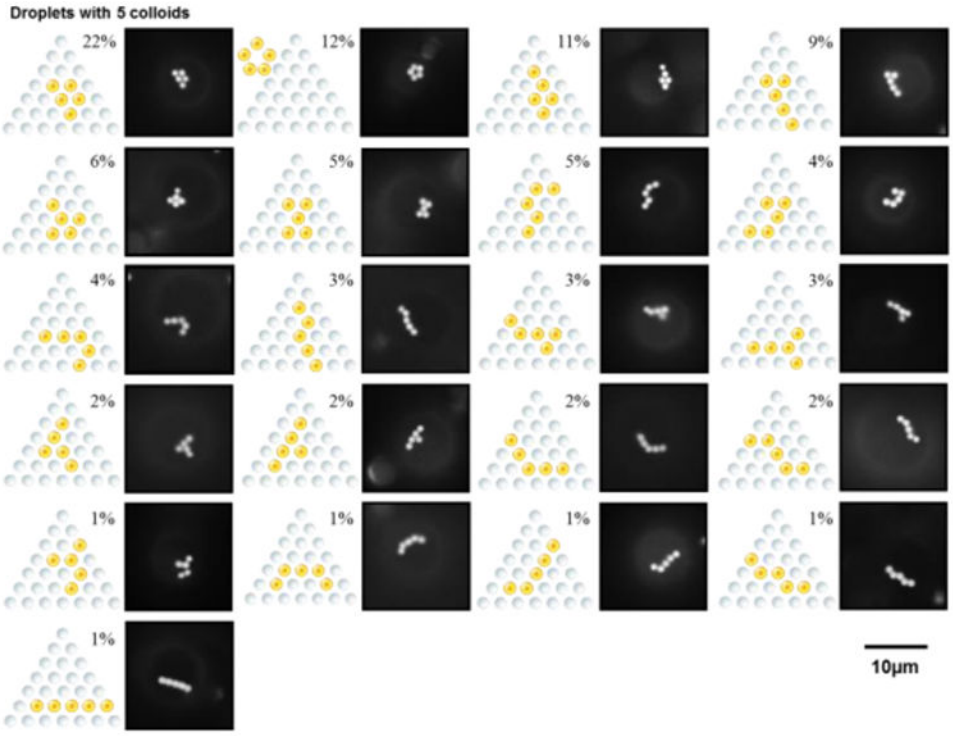

Fig. 2.

Packing arrangements observed for five PS colloids adsorbed to the poles of bipolar 5CB droplets. The percentages were calculated from analysis of 287 droplets in 5 independent experiments. In Fluo micrographs, the contrast is enhanced to highlight the arrangements of colloids.

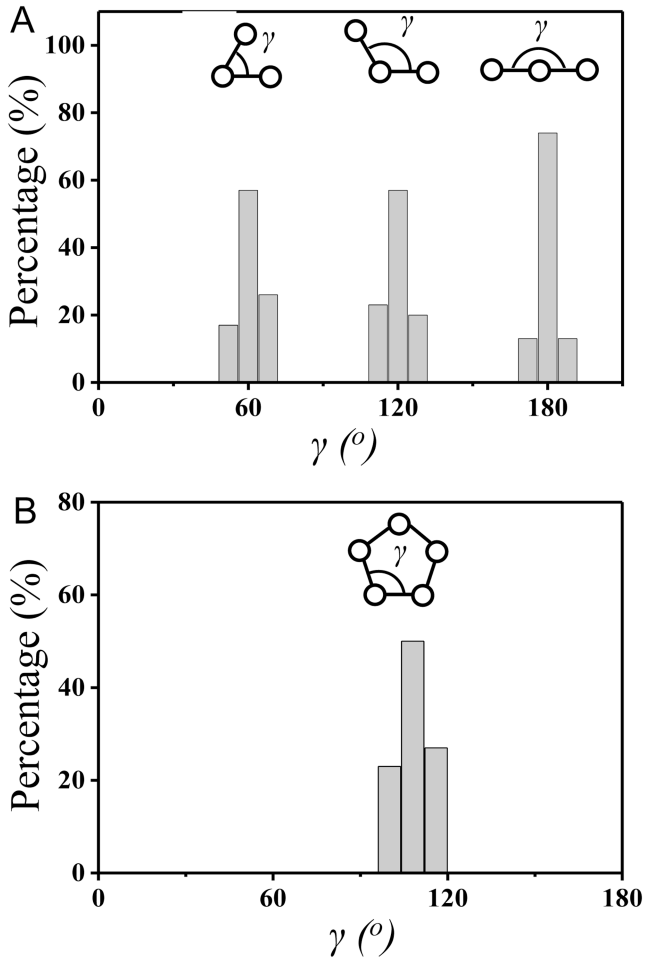

Fig. 3.

Distribution of angles (γ, see inset) defined by PS colloids adsorbed to droplets of 5CB in (A) hexagonal or (B) pentagonal arrangement. The histograms were assembled from (A) 40 or (B) 15 droplets in 3 independent experiments.

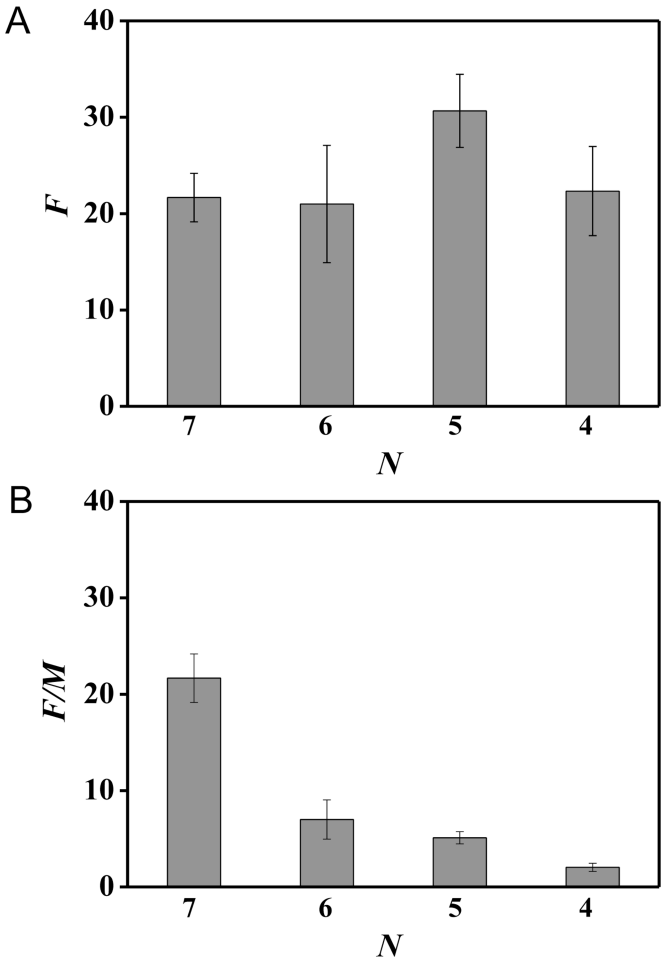

Fig. 4.

(A) Frequency (*F*) histogram of the nearest neighbor colloid—colloid contacts (*N*) in packing arrangements with five PS colloids adsorbed to poles of bipolar 5CB droplets. (B) *F* in A normalized by the multiplicity of arrangements possible for a given *N* (*M*). The plots were constructed from Fig. 2.

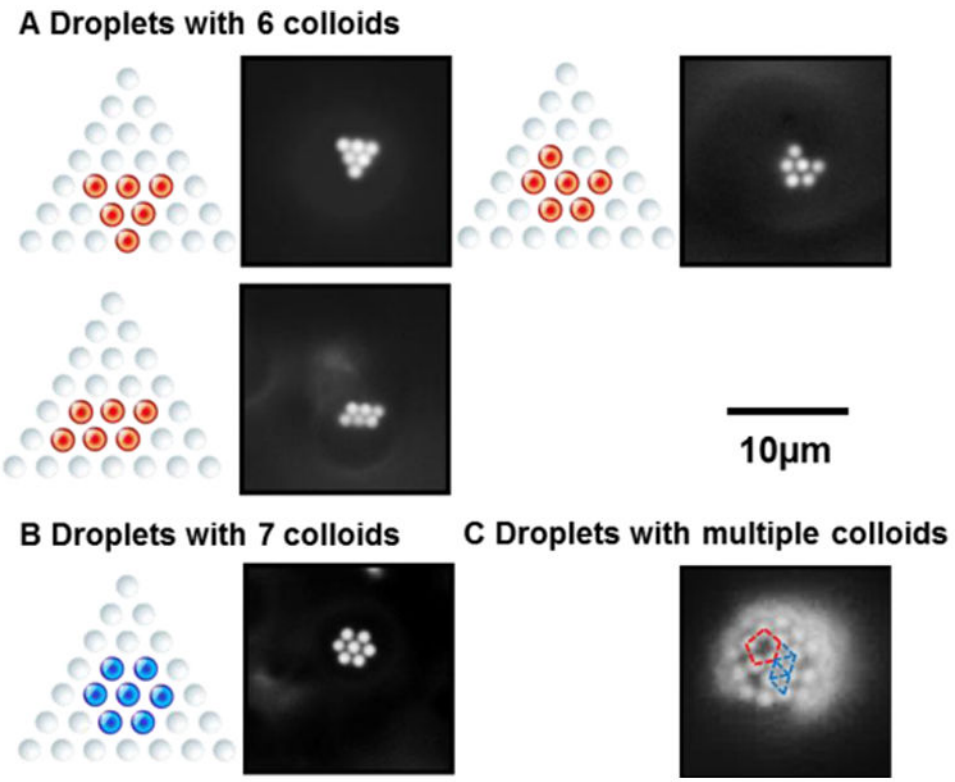

Fig. 5.

Packing arrangements most frequently observed for bipolar 5CB droplets with (A) six or (B) seven PS colloids adsorbed to their poles. (C) Packing arrangements observed for multiple PS colloids adsorbed at the surfaces of bipolar 5CB droplets. Colloids that follow a hexagonal or pentagonal pattern are marked by blue or red dashed lines, respectively. In Fluo micrographs, the contrast is enhanced to highlight the arrangements of colloids.

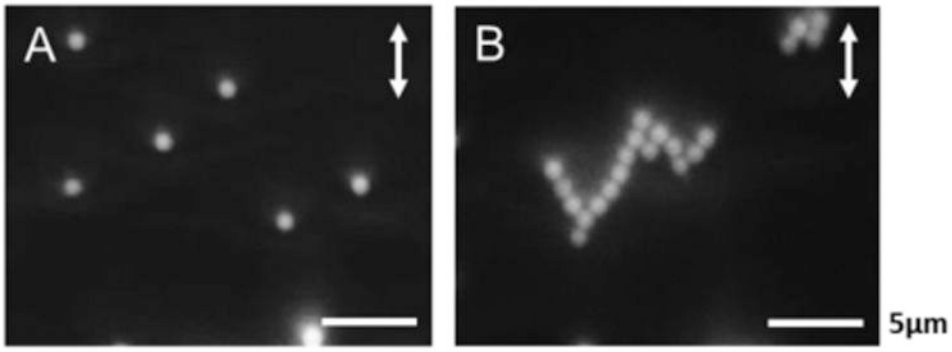

Fig. 6.

Packing arrangements observed for PS colloids adsorbed at the aqueous—LC interface of a planar 5CB film (A) in pure water or (B) in the presence of 1 mM NaCl supported on a rubbed polyimide-coated glass slide. Double headed arrows indicate the rubbing direction of polyimide.

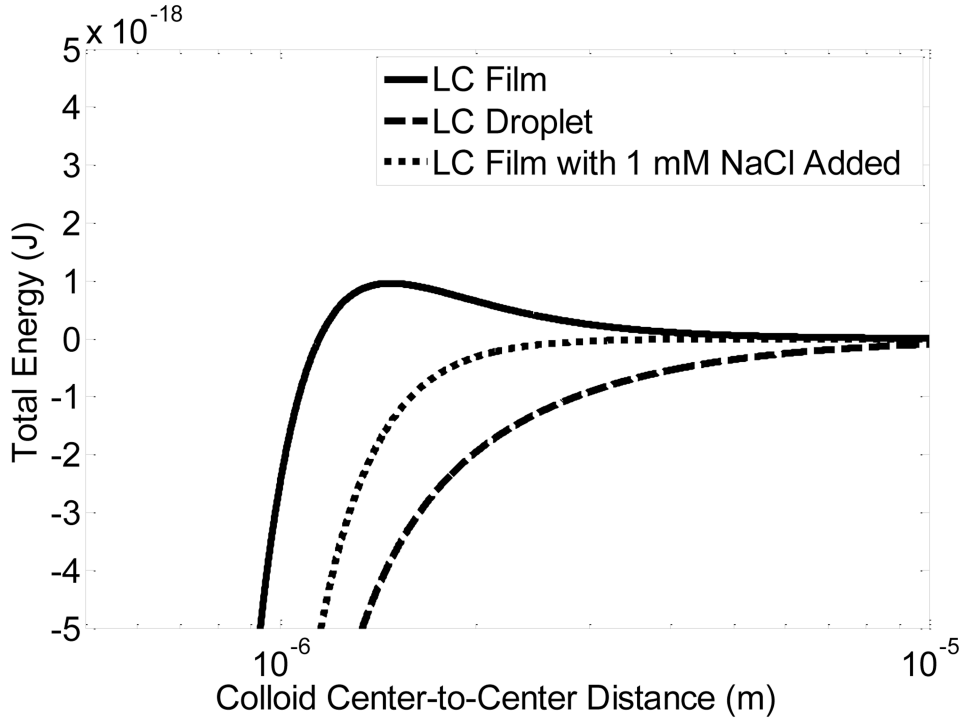

Fig. 7.

Dependence of total free energy on the center-to-center distance between PS colloids adsorbed at the aqueous—LC interface of (solid line) a planar LC film in pure water, (dashed line) a bipolar LC droplet in pure water, or (dotted line) a planar LC film in the presence of 1 mM NaCl.